BIOCHEMISTRY

 Volume 43, Number 16 April 27, 2004

Accelerated Publications

Insight into the Mechanism of the B_{12}-Independent Glycerol Dehydratase from *Clostridium butyricum*: Preliminary Biochemical and Structural Characterization‡

Jessica Rae O'Brien,§ Celine Raynaud,|| Christian Croux,|| Laurence Girbal,|| Philippe Soucaille,|| and William N. Lanzilotta*,§

Laboratorie de Biotechnologies-Bioprocédés, Toulouse, France, and Department of Biochemistry and Molecular Biology, University of Georgia, Athens, Georgia 30602

Received October 29, 2003; Revised Manuscript Received March 3, 2004

ABSTRACT: The molecular characterization of a B_{12}-independent glycerol dehydratase from *Clostridium butyricum* has recently been reported [Raynaud, C., et al. (2003) *Proc. Natl. Acad. Sci. U.S.A. 100*, 5010−5015]. In this work, we have further characterized this system by biochemical and crystallographic methods. Both the glycerol dehydratase (GD) and the GD-activating enzyme (GD-AE) could be purified to homogeneity under aerobic conditions. In this form, both the GD and GD-AE were inactive. A reconstitution procedure, similar to what has been reported for pyruvate formate lyase activating enzyme (PFL-AE), was employed to reconstitute the activity of the GD-AE. Subsequently, the reconstituted GD-AE could be used to reactivate the GD under strictly anaerobic conditions. We also report here the crystal structure of the inactive GD in the native (2.5 Å resolution, $R_{cryst} = 17\%$, $R_{free} = 20\%$), glycerol-bound (1.8 Å resolution, $R_{cryst} = 21\%$, $R_{free} = 24\%$), and 1,2-propanediol-bound (2.4 Å resolution, $R_{cryst} = 20\%$, $R_{free} = 24\%$) forms. The overall fold of the GD monomer was similar to what has been observed for pyruvate formate lyase (PFL) and anaerobic ribonucleotide reductase (ARNR), consisting of a 10-stranded β/α barrel motif. Clear density was observed for both substrates, and a mechanism for the dehydration reaction is presented. This mechanism clearly supports a concerted pathway for migration of the OH group through a cyclic transition state that is stabilized by partial protonation of the migrating OH group. Finally, despite poor alignment (rmsd ∼ 6.8 Å) of the 10 core strands that comprise the barrel structure of the GD and PFL, the C-terminal domains of both proteins align well (rmsd ∼ 0.7 Å) and have structural properties consistent with this being the docking site for the activating enzyme. A single point mutation within this domain, at a strictly conserved arginine residue (R782K) in the GD, resulted in formation of a tight protein−protein complex between the GD and the GD-AE *in vivo*, thereby supporting this hypothesis.

Radical-catalyzed reactions in biological systems are of great significance. In particular, the arrival of the genomic and proteomic era, coupled with advances in scientific methods and technology, has had a dramatic impact on our understanding of protein radicals in catalysis. Among one of the most recent developments is the recognition of a new superfamily of enzymes that utilizes *S*-adenosylmethionine (SAM) in place of adenosylcobalamin (B_{12}) to catalyze radical reactions at enzymatic sites (for reviews, see refs *1*−*4*). Despite intensive biochemical and spectroscopic investigation, the exact chemical details of radical generation

‡ Atomic coordinates for the native, glycerol-bound, and 1,2-propanediol-bound forms of the glycerol dehydratase have been deposited in the Protein Data Bank as entries 1R8W, 1R9D, and 1R9E, respectively.

* To whom correspondence should be addressed. Phone: (706) 542-1324. Fax: (706) 542-1738. E-mail: wlanzilo@bmb.uga.edu.

§ University of Georgia.

|| Laboratorie de Biotechnologies-Bioprocédés.

10.1021/bi035930k CCC: $27.50
Published on Web 04/02/2004

in this new superfamily, termed the "radical SAM" superfamily (*5*), remain unclear. Like the B_{12}-dependent reactions, this new superfamily of enzymes has been identified in all kingdoms of life and has been shown to catalyze a diverse array of chemical reactions of significant medical and biotechnological importance (*5*). It has been further suggested that the diversity of chemical reactions catalyzed by this new superfamily exceeds those catalyzed by B_{12} (*1*). Although different enzymes in the radical SAM superfamily appear to require different cofactors specific to their "primary" metabolic substrate, it appears that a common mechanism is at work in the generation of the initial radical species. The cofactors required for this common activation mechanism are a $[4Fe\text{-}4S]^{+}$ cluster (formally three Fe^{2+} ions and one Fe^{3+} ion) and *S*-adenosylmethionine (SAM). This catalytic cluster is similar to the cluster found in aconitase in that one iron is uncoordinated. The role of this open coordination site has been demonstrated by both spectroscopic and crystallographic methods and is to coordinate the SAM prior to reductive cleavage (*6*, *7*). Reductive cleavage of SAM results in the transient formation of a 5′-deoxyadenosyl radical (*8*, *9*). While this is reminiscent of the B_{12} reaction mechanism, the exact chemical details are not well understood as this radical is highly reactive and rapidly transferred to the active site where conversion of the primary metabolic substrate can proceed.

Two areas of intense research have been initiated to investigate (1) the mechanism of radical generation by the Fe−S cluster and SAM as well as (2) the general mechanism of radical transfer and catalysis during the conversion of the primary substrate to product. For some radical SAM systems, all the components necessary for activation and conversion of the primary metabolic substrate are found within a single polypeptide. In contrast, some systems require an additional enzyme for the initial radical generation. Of particular interest to this work are anaerobic ribonucleotide reductase (ARNR)[1] and pyruvate formate lyase (PFL). In these radical SAM systems, the activating enzyme contains the catalytic [4Fe-4S] cluster and the SAM binding site, while the enzyme proper contains the active site for the primary metabolic substrate. Details regarding the complex formed between these two enzymes are essential to the completion of an accurate description of the activation mechanism and the mechanism of radical transfer.

One reaction that has, until most recently, been shown to be exclusively catalyzed by B_{12} is the dehydration of glycerol to 3-hydroxylpropionaldehyde (3-HPA). In most systems, the subsequent reduction of 3-HPA to 1,3-propanediol (1,3-PD) is catalyzed by a NADH-dependent reductase. The bacterial conversion of glycerol to 1,3-PD has attracted significant interest because of the recent development of a new polyester called poly(propylene terephthalate). The polymer is essentially made by substituting 1,3-PD for ethylene glycol in producing polyester and results in a new fiber with superior properties (*10*, *11*). However, chemical processes for producing 1,3-PD involve toxic intermediates and chemical conversion under dangerous and expensive conditions. Not too surprisingly, several patents have recently been filed that describe environmentally friendly approaches for conversion of renewable resources such as glucose to 1,3-PD (*12*, *13*). All of these approaches utilize recombinant microorganisms expressing the appropriate genes to convert a renewable resource, such as glucose, to 1,3-PD. The penultimate step of this pathway is the dehydration of glycerol to 3-HPA. The mechanism of both the B_{12}-dependent glycerol and diol dehydratases has been extensively studied and is fairly well understood (*14*). A severe limitation of the B_{12}-dependent glycerol and diol dehydratases is their rapid inactivation during enzyme turnover with glycerol (*15*−*18*). This limitation is overcome in the native organism by the presence of a reactivase enzyme that couples the energy of MgATP hydrolysis to the exchange of inactivated cofactor with new coenzyme B_{12} (*19*). At present, engineered strains carrying the B_{12}-dependent system do not contain the reactivase; the inactivation problem is therefore overcome by the addition of excessive amounts of vitamin B_{12} to the culture medium. An exciting alternative has been presented by Raynaud et al. through their identification and molecular characterization of a B_{12}-independent glycerol dehydratase system from the strict anaerobe *Clostridium butyricum*. Like the B_{12}-dependent glycerol dehydratases, this system was also capable of dehydrating 1,2-propanediol to propionaldehyde in addition to glycerol dehydration (*20*). Further sequence analysis of this operon suggested that this system was also a member of the radical SAM superfamily. Specifically, this system was similar to PFL in that it contained genes for the glycerol dehydratase (GD) as well as a glycerol dehydratase activating enzyme (GD-AE).

To further advance our understanding of the radical SAM superfamily as well as to accurately describe a mechanism for the B_{12}-independent dehydration of glycerol, we have further isolated the B_{12}-independent GD and GD-AE. We report here the preliminary biochemical properties of this system as well as the crystallographic models for the radical-free form of the GD in the absence of substrate and with the substrates glycerol and 1,2-propanediol bound. A detailed mechanism for the B_{12}-independent dehydration of glycerol is presented. In addition, the ability to follow the activity of the system *in vivo* and rapidly isolate either component has led to the identification of a single point mutation in the GD that forms a tight complex with the GD-AE. Taken together, the work presented here provides the first direct evidence for the site of complex formation in the two-component radical SAM systems and the first look at the atomic factors that catalyze B_{12}-independent glycerol dehydration in biology.

EXPERIMENTAL PROCEDURES

Plasmid Preparation and Enzyme Expression. The polycistronic plasmids used for coexpression of the glycerol dehydratase (GD) and the glycerol dehydratase activating enzyme (GD-AE) from *C. butyricum* were prepared as previously described (*20*), except that 11 additional residues (MWSHPQFEKRS) were added to the N-terminus of either the GD (plasmid pST11) or the GD-AE (plasmid pST12). This epitope is more commonly known as the Strep-Tag

[1] Abbreviations: TRIS, tris(hydroxymethyl)aminomethane; TCEP, tris(2-carboxyethyl)phosphine hydrochloride; HEPES, *N*-(2-hydroxyethyl)piperazine-*N*′-2-ethanesulfonic acid; GD, glycerol dehydratase; GD-AE, glycerol dehydratase activating enzyme; PFL, pyruvate formate lyase; PFL-AE, pyruvate formate lyase activating enzyme; LAM, lysine amino mutase; LAM-AE, lysine amino mutase activating enzyme; ARNR, anaerobic ribonucleotide reductase; ARNR-AE, anaerobic ribonucleotide reductase.

(IBA, Göttingen, Germany) and is used for affinity purification. Like their parent plasmids (pSPD5 and pIMP1), the expression plasmids also carry the *dhaT* gene that encodes the 1,3-propanediol dehydrogenase. Consistent with what has also been previously reported (*20*), conversion of glycerol to 1,3-propanediol was observed during the anaerobic growth of *Escherichia coli* cells harboring either of these plasmids.

While the pST11 plasmid was sufficient for the isolation of the GD (~10 mg of pure enzyme from 20 g of wet cell paste), relatively small amounts of the GD-AE were obtained using the pST12 plasmid (<1 mg of pure enzyme from 50 g of wet cell paste). To obtain better expression of the GD-AE, the *dhaB2* gene was amplified using PCR methods, and the primers were designed to incorporate *Nhe*I and *Hin*dIII restriction sites at the 5′ and 3′ ends of the gene, respectively. The PCR product was then subcloned into the commercially available expression vector pTRCHisA (Invitrogen Corp., Carlsbad, CA). Instead of the Strep-Tag, this vector incorporates a six-poly-His tail at the N-terminal end of the GD-AE.

Purification of the GD. The following procedures could be performed under either aerobic or anaerobic conditions. When the procedure was performed under anaerobic conditions, *E. coli* cells harboring the pST11 plasmid were grown on LB medium supplemented with nitrilotriacetic acid (200 mg/L), $FeSO_4$ (50 mg/L), K_2HPO_4 (0.5 g/L), sodium selenate (30 μg/L), and glycerol (40 g/L). A 50 mL overnight culture was used to inoculate a 2000 mL culture that was contained in a 4000 mL glass carboy. Following inoculation, the carboy was sealed with a screw cap and the culture was incubated at 34 °C and 110 rpm for 18 h. The cells were harvested anaerobically by centrifugation and stored at −80 °C. In addition, for anaerobic purifications, all buffers were made anaerobic by several rounds of degassing and flushing with oxygen-scrubbed argon and contained 1 mM Ti(III) citrate. All subsequent purification procedures were then performed in a glovebox under an atmosphere of 95% nitrogen and 5% hydrogen.

Approximately 50 g of wet cells was resuspended in 350 mL of buffer A [150 mM NaCl, 2 mM TCEP, and 50 mM TRIS (pH 8.0)]. Cells were then broken at 16 000 psi using a French press. The pellet was then discarded, and 5 mg of avidin (Sigma, St. Louis, MO) was added to the supernatant. The supernatant was then gently stirred for an additional 30 min at 4 °C before being centrifuged at 10 000 × *g* for 10 min. This supernatant was passed through a Strep-Tactin Sepharose (IBA) column that had been equilibrated with buffer A. Once the supernatant was loaded onto the column, the column was then washed with 20 volumes of buffer A. Buffer A containing 2.5 mM *d*-desthiobiotin (Sigma) was then used to elute the bound protein. The purified protein was then exchanged into fresh buffer A and concentrated to 10 mg/mL.

Isolation and Reconstitution of the GD-AE. Inactive GD-AE was isolated using the Talon metal affinity resin (Clonetech, Palo Alto, CA). Fifty grams of wet cells was resuspended in buffer containing 20% 1,2-propanediol, 100 mM HEPES (pH 7.5), and 100 mM KCl (buffer B). The resuspended cells were broken using a French press at 16 000 psi and centrifuged at 50 000 × *g* for 1 h. The supernatant was then applied to affinity resin equilibrated with buffer B. The column was then washed with 20 column volumes of buffer B, and the bound GD-AE was eluted with buffer B containing 150 mM imidazole. The isolated enzyme was immediately degassed on an argon manifold and concentrated to 1−2 mL. In this form, the GD-AE was unable to activate the GD.

To reconstitute the GD-AE activity, we employed the same procedure used for PFL-AE (*21*) except that the Mops buffer was replaced with HEPES and the reconstitution buffer also contained 20% 1,2-propanediol. An incubation time of 12 h was used for reconstitution, and the reconstituted GD-AE was separated from excess iron and sulfide by being passed through a Sephadex G25 column equilibrated with 100 mM HEPES (pH 7.5), 100 mM KCl, 2 mM mercaptoethanol, and 2 mM sodium dithionite. The reconstituted GD-AE was concentrated to 1 mL. Typical yields for the entire isolation and reconstitution procedure were 20 mg of GD-AE from 50 g of wet cell paste. All enzymes used in this study were homogeneous as judged by SDS−PAGE, and their concentrations were determined by a modified biuret method (*22*).

Activation of the GD by the GD-AE. It has been previously reported (*20*) that this system, like the B_{12}-dependent glycerol dehydratases, can also catalyze the dehydration of 1,2-propanediol to propionaldehyde. To test the ability of the GD-AE to reactivate the GD, we modified a procedure that had been previously reported (*20*). The assay was performed under strictly anaerobic conditions in sealed quartz cuvettes at 25 °C, and the final assay volume was 0.5 mL. The assay solution contained 5% 1,2-propanediol, 100 mM HEPES (pH 7.5), 1.13 μM GD, 1 mg/mL yeast alcohol dehydrogenase (YADH) (Sigma Chemical Co., lot 070K7432), 220 μM NADH, and 2 mM sodium dithionite. This solution was prepared with and without 5 mM SAM. Before the assay was initiated, the spectrophotometer was blanked against buffer containing 100 mM KCl, 100 mM HEPES (pH 7.5), and 2 mM sodium dithionite. The assay was initiated by addition of varying amounts of purified GD-AE, and the absorbance at 340 nm was monitored. The GD-AE used in this study was purified as described above and concentrated to a final concentration of 18 mg/mL prior to being used in the assay.

Crystallization of the GD. The best diffracting crystals of the GD were obtained using aerobically prepared protein and a precipitating solution containing 200 mM triammonium citrate (pH 7.0) and 10% PEG 3350. Diffraction quality crystals could be obtained under anaerobic or aerobic conditions using either the capillary batch or hanging drop method. Crystals of the GD belonged to space group $C222_1$ and had the following unit cell dimensions: $a = 104$ Å, $b = 212$ Å, and $c = 199$ Å (see Table 1). These crystals were taken to be the substrate free GD crystals. These crystals could be soaked with up to 20% glycerol (glycerol-bound crystals) or 20% 1,2-propanediol (1,2-propanediol-bound crystals) without any significant changes in the diffraction quality. For data collection on the native or substrate-free form of the enzyme, crystals were mounted in quartz capillaries and data were collected at room temperature.

Data Collection, Phasing, Model Building, and Refinement. Data for the substrate-free GD and the 1,2-propanediol-bound form of the GD were collected at the University of Georgia on a Rigaku RU-200 rotating anode equipped with Osmic focusing mirrors and an R-axisIIc image plate detector. Data for the glycerol-bound form of the GD were

Table 1: Data Collection, Phasing Statistics, and Refinement Statistics for the Native Glycerol Dehydratase and Its Substrate-Bound Forms

	native glycerol-free	glycerol-bound	1,2-propanediol-bound	Hg derivative
no. of crystals used	5	1	1	5
wavelength (Å)	1.54	0.98	1.54	1.54
resolution range (Å)	50.0−2.5	50.0−1.8	50.0−2.4	50.0−2.5
no. of unique observations	74994	199038	83330	73024
total no. of observations	427249	1002737	491798	422078
completeness (%)	98.6 (93.5)[b]	99.5 (96.5)[b]	98.0 (90.8)[b]	96.9 (90.3)[b]
R_{sym} (%)[a]	9.9 (38.5)[b]	8.3 (28.2)[b]	9.6 (31.2)[b]	12.7 (44.7)[b]
I/σ	29.7 (2.2)[b]	26.7 (3.3)[b]	20.0 (3.2)[b]	27.8 (1.7)[b]
R_{cullis} (cen/acen/anom)				0.84/0.80/0.81
phasing power (cen/acen/anom)				1.24/1.47/1.45
isomorphous difference (%)				27.8
no. of sites				8

	substrate-free	glycerol-bound	1,2-propanediol-bound
unit cell dimensions (Å)[c]	$a = 103.4$, $b = 212.9$, $c = 199.4$	$a = 103.0$, $b = 213.4$, $c = 199.5$	$a = 102.6$, $b = 212.3$, $c = 198.7$
no. of protein atoms	12370	12390	12392
no. of solvent atoms	511	969	696
resolution limits (Å)	50.0−2.5	50.0−1.8	50.0−2.4
R_{cryst} (%)	17.1	21.7	19.8
R_{free} (%)	20.3	23.8	23.5
rmsd for bonds (Å)	0.005	0.005	0.005
rmsd for main chain angles (deg)	1.21	1.21	1.19
average B factor (Å^2)	28.4	31.1	27.0

[a] $R_{sym} = \sum_{hkl}[\sum_I(|I_{hkl,I} - \langle I_{hkl}\rangle|)]/\sum_{hkl,I}\langle I_{hkl}\rangle$, where I_{hkl} is the intensity of an individual measurement of the reflection with indices *hkl* and $\langle I_{hkl}\rangle$ is the mean intensity of that reflection. [b] The numbers in parentheses refer to the outer resolution bin used in data processing. [c] Space group $C222_1$ so all angles are 90°.

collected at the Advanced Light Source (Berkeley, CA) on beamline 8.2.2. All data were processed using HKL2000 (*23*) and the CCP4 suite of programs (*24*). While both glycerol and 1,2-propanediol are excellent cryoprotective agents, we were interested in comparing the data between the substrate-free enzyme and the glycerol- or 1,2-propanediol-bound enzyme. Therefore, to collect data for both the substrate-free and a mercury derivative, data were collected at room temperature on crystals mounted in quartz capillaries. Under these conditions, approximately 30 frames worth of data could be collected before the diffraction deteriorated. Five different crystals were used to complete the data sets for both the native (substrate-free) and Hg derivative data sets. A heavy atom derivative was used for phasing because, despite the conserved sequences shared between PFL and the GD (∼23.0% identical), attempts to obtain phases by molecular replacement were unsuccessful. Because of the high cysteine content of the GD (14 cysteines per monomer), a single Hg derivative was sufficient for obtaining phase information good to 2.5 Å resolution, and therefore, no phase extension was required prior to model building and refinement (Table 1). Subsequent rounds of model building and refinement were performed using O (*25*) and CNS (*26*). All graphical representations of structural elements were made using Molscript (*27*), Bobscript (*28*), and Raster3d (*29*).

RESULTS AND DISCUSSION

Isolation of the Glycerol Dehydratase (GD) from C. butyricum and Activation of the GD by the GD-AE. Expression and isolation of the GD could be performed under both aerobic and anaerobic conditions. However, as was previously reported by Raynaud et al., to observe any activity *in vivo* or in crude extracts, *E. coli* cells expressing both the GD gene (*dhaB1*) and the GD-AE gene (*dhaB2*) had to be grown under strictly anaerobic conditions using a modified medium containing glycerol (*20*). Using the Strep-tactin Sepharose affinity resin, the GD could be isolated from aerobically grown cells under aerobic conditions or anaerobically grown cells under anaerobic conditions. However, if an aliquot of the elution fraction from the anaerobically prepared enzyme was removed from the glovebox and immediately exposed to air, then a cleavage product was observed. This is shown in Figure 1 and is reminiscent of the oxygenolytic cleavage of activated PFL (*30*). Therefore, to ensure that we had a homogeneous population of enzyme for crystallization trials, all of the GD used in the biochemical and crystallographic work was expressed and purified by aerobic methods. In this state, the enzyme is inactive, presumably because it does not contain the active site radical. The aerobic isolation of the GD-AE is also shown in Figure 1.

To test whether the GD used in this investigation could be activated by the GD-AE, we developed a simple assay based on the observation of Raynaud et al. that the system was also capable of dehydrating 1,2-propanediol to propionaldehyde. This is a coupled assay that utilizes a 10-fold excess of yeast alcohol dehydrogenase (YADH) to catalyze the NADH-dependent conversion of propionaldehyde to 1-propanol. The coupled reaction is monitored at 340 nm, and the results from these preliminary studies are shown in Figure 2. Following the addition of the GD-AE, a delay was observed prior to a decrease in the absorbance at 340 nm. No decrease was observed if either SAM or the GD-AE was excluded from the assay. Interestingly, the maximum activity was achieved once the GD-AE:GD ratio exceeded 10. Two important pieces of information must be considered in interpreting our data. First, our assay does not utilize the light-activated reductant 5′-deazariboflavin, as has been routinely used for PFL-AE (*21*). Second, it has been shown

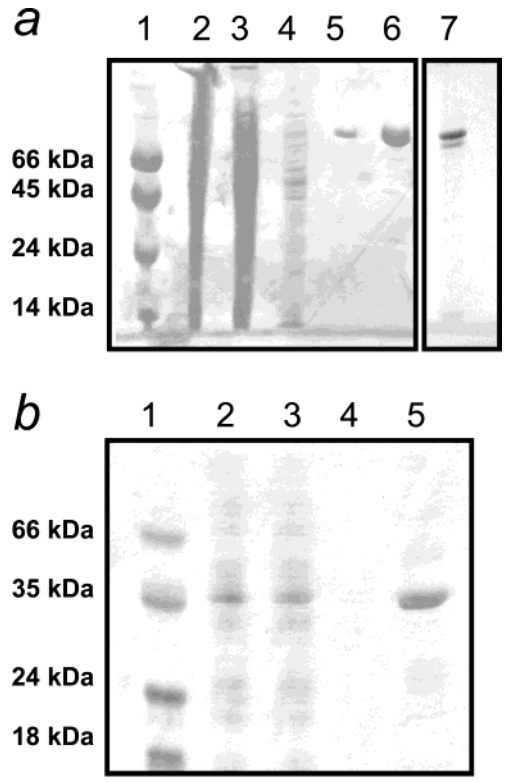

FIGURE 1: Isolation of the GD and the GD-AE. (A) Isolation of recombinant GD under aerobic conditions and effect of oxygen exposure on the activated enzyme: lane 1, molecular mass markers; lane 2, crude extract from aerobic preparation; lane 3, flow-through from the Strep-Tactin Sepharose column (aerobic preparation); lane 4, wash fraction after 10 column volumes of buffer A (aerobic preparation); lanes 5 and 6, first and second elution fractions, respectively, using buffer A containing 2.5 mM *d*-desthiobiotin (aerobic preparation); and lane 7, GD isolated under strictly anaerobic conditions from anaerobically grown *E. coli* expressing both the GD and the GD-AE after a 5 min exposure to air. (B) Isolation of recombinant GD-AE under aerobic conditions: lane 1, molecular mass markers; lane 2, crude extract; lane 3, flow-through from Talon metal affinity resin during the load; lane 4, wash fraction after 10 column volumes of buffer B; and lane 5, elution fraction using buffer B containing 150 mM imidazole.

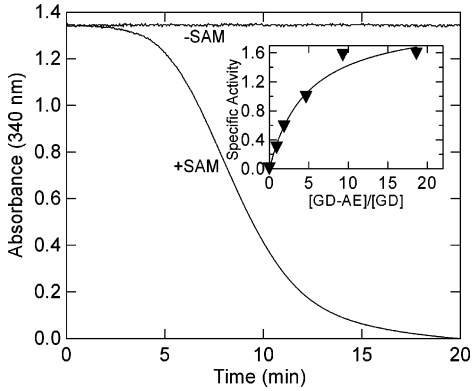

FIGURE 2: *S*-Adenosylmethionine (SAM)-dependent activation of the GD by the GD-AE. The coupled assay was performed as described in Experimental Procedures. The absorbance at 340 nm was monitored to follow the NADH-dependent reduction of propionaldehyde formed by GD-catalyzed dehydration of 1,2-propanediol (+SAM). No change in the absorbance was observed if SAM was left out of the assay solution (−SAM). The inset shows the effect of the GD-AE concentration on the activation of the GD. The specific activity was calculated from the maximum slope of the coupled assay using 6.2 mM^{-1} cm^{-1} as the molar extinction coefficient for NADH.

that activation of PFL by the PFL-AE requires an intact $[4Fe\text{-}4S]^+$ cluster to catalyze the reductive cleavage of SAM and generate the catalytic radical on PFL (*31*). At this time, we do not know if sodium dithionite is sufficient for reduction of the catalytic Fe−S cluster in the GD-AE. Moreover, at present, we do not know if the reconstitution procedure has restored the catalytic Fe−S cluster in 100% of the apo-GD-AE. In addition, the sequence of the GD-AE suggests that a second cluster is also present in the enzyme (*20*). The exact role of this second cluster has not been characterized in any radical SAM system. However, it should be noted that a second cluster binding site has also been identified in the sequences of TutE and BssD; these are also radical SAM enzymes involved in the benzyl succinate synthase system from two *Thauera* species (*32*, *33*). We are currently investigating the properties of the activated GD-AE to address these issues. What can be said is that the reconstituted GD-AE can catalytically reactivate the GD in a SAM-dependent manner. A maximum specific activity for the GD of 1.56 ± 0.09 mmol min^{-1} mg^{-1} is obtained when the ratio of GD-AE to GD exceeds 10 in our assay. Because glycerol is both a good substrate and a potent inhibitor of the B_{12}-dependent glycerol dehydratase (*34*), a comparison of the 1,2-propanediol dehydratase activity in the two systems is valid. Interestingly, the specific activity we have observed for the B_{12}-independent system is approximately 13 times that of the B_{12}-dependent glycerol dehydratase (*35*). Moreover, this specific activity also exceeds that typically reported for the B_{12}-dependent diol dehydratases (*15*, *16*, *36*). The biochemical parameters for glycerol dehydration are currently being pursued by this laboratory using purified DhaT in place of YADH in the coupled assay.

Overall Structure of the Glycerol Dehydratase Monomer. To provide a solid foundation for future biochemical and biophysical investigations, we have determined the crystal structure of the B_{12}-independent GD in the native, glycerol-bound, and 1,2-propanediol-bound forms. In all of the structures reported here, the complete translated peptide (residues 2−787) is clearly visible in the electron density. The overall structure of the GD is shown in Figure 3. Like PFL and ARNR, the GD monomer forms a core 10-stranded β-barrel motif that is assembled in an antiparallel manner from two parallel five-stranded β-sheets. This β-barrel core is entirely surrounded by α-helices as was also reported for PFL and ARNR and has been termed a β/α-barrel structure. Despite the observation of a highly conserved core, if the 10 strands that compose this motif are aligned between PFL (PDB entry 1H16) and the GD, then a root-mean-square deviation (rmsd) of 6.8 Å is obtained for the backbone α-carbon atoms. In addition to the significant variation in the core motif, there are also dramatic differences in the number and position of the surrounding helices. If the conserved helical regions are also included in this alignment, the rmsd for backbone α-carbon atoms is substantially worse (>8.0 Å). A substantial finding of this work is the observation that the only region of the GD that aligns well with PFL is the C-terminal domain (exploded view, Figure 3A). For PFL and the GD, this includes residues 731−782 (GD) and residues 702−754 (PFL), respectively. Alignment of this domain results in an rmsd of 0.7 Å for the backbone α-carbon atoms. This domain is highlighted in yellow in Figure 3 and

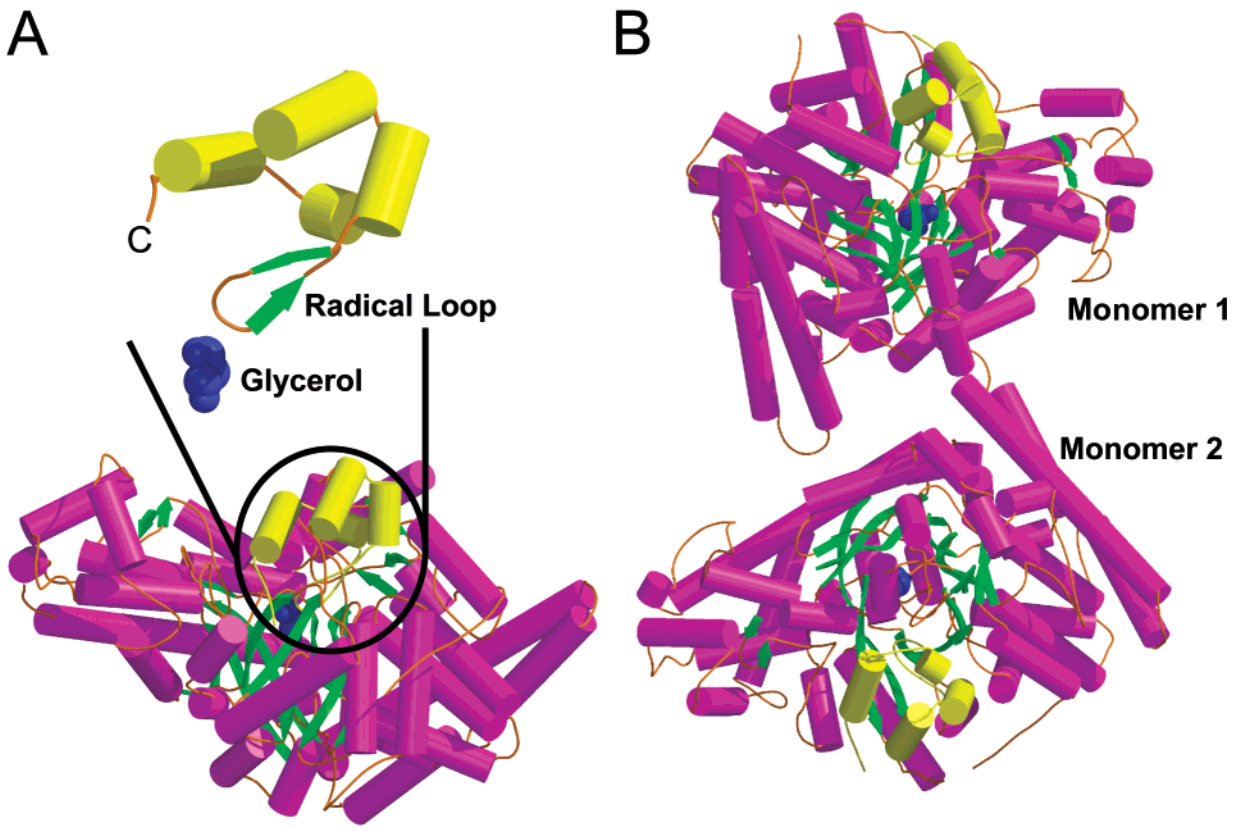

FIGURE 3: Overall fold of the glycerol dehydratase (GD) monomer and the proposed biological dimer. Helices are shown as purple cylinders; the sheet structure is represented with green strands, and random coil is represented with orange coils. The topology of the C-terminal region (residues 731−787) is represented similarly, but is colored yellow in the monomer and dimer representations. (A) Overall topology of the monomer and exploded view of the C-terminal region of the enzyme. (B) Proposed biological dimer of the GD. For clarity, monomer 1 and monomer 2 are labeled.

contains the radical glycine loop, a small antiparallel sheet section, and four helices. Notably, two of the helices are on the surface of the enzyme. This domain can therefore be described as extending from the surface of the protein to the substrate binding site at one end of the 10-stranded β-barrel.

Oligomeric Structure and a Potential Site for Binding of the Activating Enzyme. Like the most recent model of PFL (*37*), our GD crystals also belong to space group $C222_1$ and contain two monomers in the asymmetric unit. Like PFL, the two monomers are related by a nearly perfect 2-fold rotation and represent the closest contact between any two monomers in the unit cell with a buried surface area that exceeds 1000 Å^2 per monomer. Consistent with what has been proposed for PFL, we propose that this arrangement also represents the biological dimer (monomers 1 and 2 in Figure 3B). Further efforts to investigate whether the GD exists as a dimer in solution and whether this oligomeric arrangement has any impact on function are currently being pursued by this laboratory. However, if this is the correct biological dimer, then the C-terminal domain of each monomer is found on the opposite side of the dimer interface. One significant property that both the GD and PFL have in common is that they must be activated by another enzyme. This involves docking of the activating enzyme, and therefore, a significant unanswered question is the site of complex formation. Given (i) the overall structural similarities of PFL and the GD, (ii) the observation that a similar reconstitution procedure can be used to reconstitute the PFL-AE as well as the GD-AE, and (iii) the observation that the only region of PFL and the GD that aligns well is the C-terminal domain, we propose that this is the site of formation of the complex between the activating enzyme and the enzyme proper in both systems. To further examine this hypothesis, a sequence and structural alignment of this domain between PFL and the GD is shown in Figure 4. All of the side chains that are shown in Figure 4 are strictly conserved between PFL and the GD and are further found in identical conformations in both crystallographic models. Of particular interest is the *cis* conformation of the strictly conserved glycine residue. Another noteworthy residue that is strictly conserved in sequence and structure is R782 in the GD (R753 in PFL). In the structure of the GD and PFL, this residue extends inward from the C-terminal helix to form a hydrogen bond with the backbone carbonyl of a residue that is only two amino acids away from the active site glycine (dashed lines in Figure 4, ~2.9 Å). Again, in both crystallographic models, this interaction is further stabilized through a salt bridge to an acidic residue found within the same C-terminal helix. The distance from the surface of the GD to the active site along this pathway is ~17 Å; however, in both the PFL and GD models, a substantial amount of water molecules are clearly seen on the interior side of this helix. This observation may suggest that this helix moves during activation. Further evidence for this hypothesis comes from the single-point mutation R782K in the GD.

During our initial attempts to construct the pST12 plasmid, a single-point mutation was serendipitously introduced into the GD gene, and sequence analysis confirmed that AAG was substituted for AGG in the codon for residue 782.

```
GD  731-GFHVQFNVIDKKILLAAQKNPEKYQDLIVRVAGYSAQFISLDKSIQNDIIART-783
PFL 703-GQHLNVNVMNREMLLDAMENPEKYPQLTIRVSGYAVRFNSLTKEQQQDVITRT-754
```

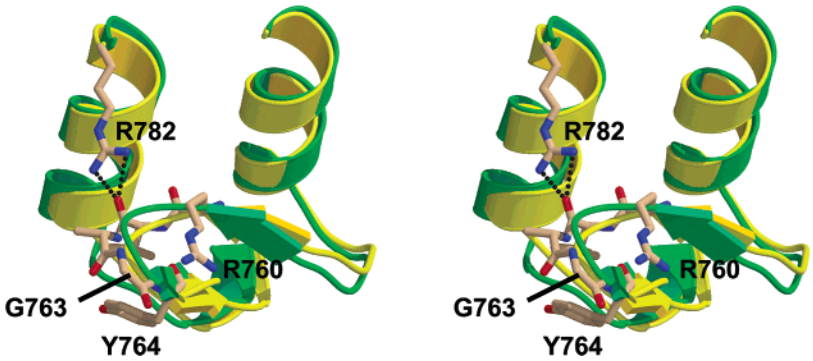

FIGURE 4: Sequence and structural comparison of the C-terminal domains of PFL and the GD. Identical residues are colored red and similar residues blue in the sequence alignment. The structural topology of residues in the sequence alignment is shown in a stereoview with PFL colored green and the GD colored yellow. The side chains of strictly conserved residues in the GD model are represented as balls and sticks with the carbon atoms colored light brown, oxygen atoms colored red, and nitrogen atoms colored blue. The side chain of R782 comes within 3.0 Å of the backbone carbonyl oxygen of residue 761 (dotted line).

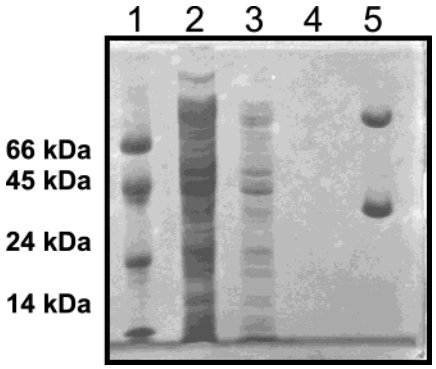

FIGURE 5: Isolation of a tight protein−protein complex between the GD-AE and the R782K GD *in vivo*: lane 1, molecular mass markers; lane 2, crude extract from *E. coli* cells harboring the pR782KGD-ST12 plasmid; lane 3, first wash fraction; lane 4, last wash fraction; and lane 5, elution fraction.

Sequence analysis also confirmed that the sequence for the affinity-tagged GD-AE was correct. Since the point mutation was on the GD and the Strep-Tag was on the GD-AE, we thought that this plasmid (pR782KGD-ST12) might still be useful for production of wild-type GD-AE as well as in investigating the impact of this point mutation on the *in vivo* activity of the glycerol dehydratase system. Surprisingly, no activity could be detected in crude extracts or *in vivo* for this construct. As was observed for the parent plasmids (*20*), reconstruction of this plasmid (without the R782K point mutation) resulted in full activity *in vivo*. To further confirm that the loss of activity was due to the R782K point mutation in the GD and not the affinity tag on the N-terminus of the GD-AE, we have shown in Figures 1 and 2 it is possible to isolate the affinity-tagged GD-AE and use it to activate the wild-type GD. We then took a step backward and attempted to isolate the GD-AE anaerobically from crude extracts of *E. coli* cells harboring the pR782KGD-ST12 plasmid that were grown under the conditions described previously (*20*). The results of this purification are shown in Figure 5. Despite the fact that the affinity tag is on the GD-AE, both the GD and the GD-AE eluted from the column after the column had been washed with several column volumes of buffer. These data suggest that a tight protein−protein complex has been formed *in vivo* as a result of the R782K point mutation on the GD. This observation further supports our hypothesis that this region is the site of formation of a complex between the GD and the GD-AE. The factors that are required for formation of the complex are currently being investigated by isolating the R782K GD and wild-type GD-AE independently and then initiating complex formation *in vitro*. An exciting possibility is that the complex forms after electron transfer and radical generation and that this arginine residue has a role in dissociation. Structural and spectroscopic characterization of such a complex with the radical intact would be extremely valuable.

Substrate Binding. Because both glycerol and 1,2-propanediol have been shown to be good substrates for the GD (*20*), the interaction of both of these substrates was investigated. The binding mode of glycerol is shown in Figure 6. A number of hydrogen bonds position the glycerol molecule so that both of the terminal carbon atoms are each 3.7 Å from the γ-sulfur atom of the active site cysteine (C433). This residue is strictly conserved in PFL and ARNR. For PFL, Kozarich and co-workers have shown that a thiyl radical is generated at this site as a result of hydrogen atom abstraction by the active site glycyl radical (*38*). Comparison of the substrate-free and substrate-bound form of the GD suggests that there is some movement of the γ-sulfur atom of C433 toward the α-carbon atom of G763 as this distance is 4.4 Å in the substrate-free structure and 4.0 Å in the glycerol-bound structure. A thiyl radical on the γ-sulfur atom of C433 would be perfectly positioned to abstract a hydrogen atom from either end of the glycerol. The question of which end of the substrate is the site of hydrogen atom abstraction arises. This is easily answered by examining the binding mode of the alternative substrate 1,2-propanediol. The binding mode of 1,2-propanediol is shown in Figure 7. Of particular interest is the purple density, which essentially represents the missing OH group when the 1,2-propanediol and glycerol data are compared. These data clearly place the 1-OH group of 1,2-propanediol in a hydrogen bond with the carboxylic acid oxygen of E435 (2.6 Å). At the opposite end of either substrate, a direct connection between the bulk solvent and the active site is observed. This is accomplished

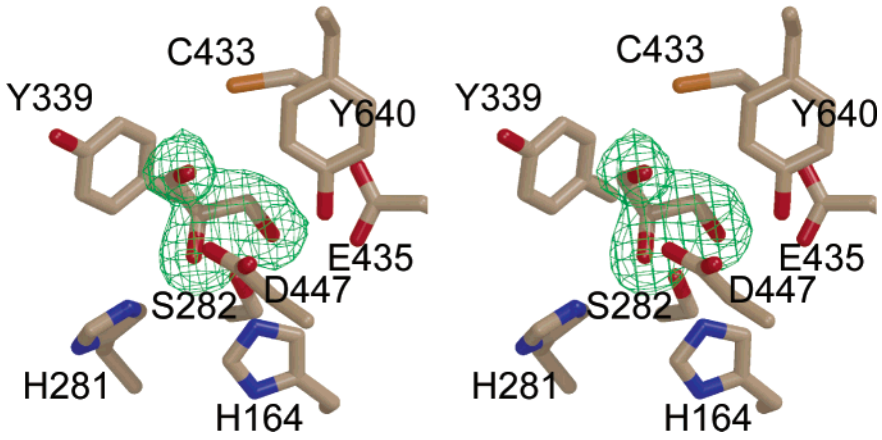

FIGURE 6: Stereoview of the active site with glycerol bound. All atoms are represented by ball-and-stick models with the carbon atoms colored light brown, oxygen atoms colored red, nitrogen atoms colored blue, and sulfur atoms colored orange. The green cage represents a Fourier difference ($F_o - F_c$) map contoured at 4σ using the observed glycerol-bound structure factors and the calculated phases from the substrate-free model.

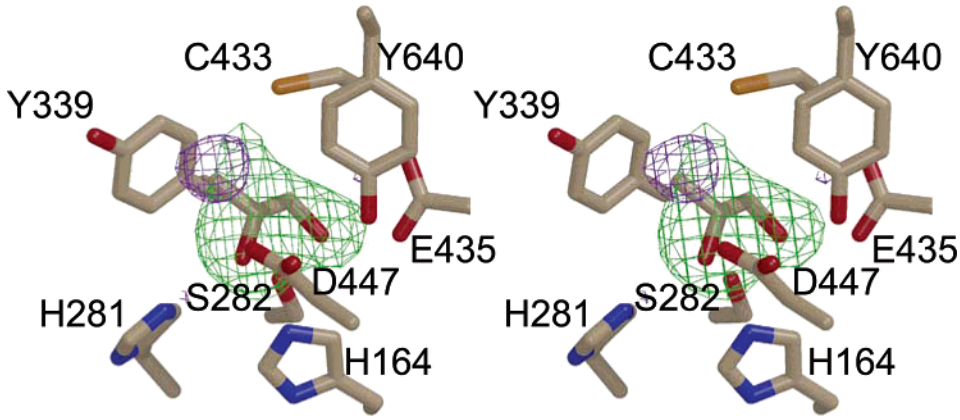

FIGURE 7: Stereoview of the active site with 1,2-propanediol bound. All atoms are represented by ball-and-stick models with the carbon atoms colored light brown, oxygen atoms colored red, nitrogen atoms colored blue, and sulfur atoms colored orange. The green cage represents a Fourier difference ($F_o - F_c$) map contoured at 4σ using the observed 1,2-propanediol-bound structure factors and the calculated phases from the substrate-free model. The purple cage represents a Fourier difference ($F_o - F_c$) map contoured at 4σ using the observed glycerol-bound structure factors and the calculated phases from the 1,2-propanediol-bound model.

through a series of hydrogen-bonded water molecules that extend from the side chain of D447 to the surface of the enzyme and into the bulk solvent.

Mechanism of B_{12}-Independent Glycerol Dehydration. Given the structural details revealed here and the extensive information available for the B_{12}-dependent glycerol and diol dehydratases, a reasonable hypothesis for the B_{12}-independent mechanism of glycerol dehydration can be surmised. Given that the GD system is structurally similar to PFL and the observation that the activation of the GD by the GD-AE is SAM-dependent, we propose that the activation mechanism will be similar to that of PFL, specifically, that activation of the GD by the GD-AE will result in a stable glycyl radical at G763 and that this radical will be in equilibrium with a thiyl radical at the γ-sulfur atom of C433. Whether this is the case, and the mechanism of propagation of a radical from the GD-AE to the active site of the GD, are currently under investigation. In particular, the observation that the key glycine residue is structurally conserved in the models of the GD, ARNR, and PFL would suggest that these enzymes all share a common activation mechanism. While PFL appears to require two cysteine residues (C418 and C419) for activity, only one of these residues (C419) is conserved in the sequence and structures of the GD and ARNR. This would be equivalent to C433 in the GD and would represent the site of the thiyl radical. Therefore, our proposed mechanism for B_{12}-independent glycerol dehydration is shown in Figure 8, and begins at the point where, by analogy with PFL, the active site glycyl radical has already abstracted a hydrogen atom from the γ-sulfur atom of C433.

The binding modes of the substrates examined here indicate that a thiyl radical at C433 would be perfectly positioned to abstract the *pro-S* hydrogen atom from C1 of either substrate. A significant mechanism for lowering the activation barrier for this event may come from the resonance of the peptide bond between residue 433 and residue 434. Since the amide proton of this peptide is hydrogen bonded to the acidic side chain of E435, the strength of this hydrogen bond is associated with the overall resonance of the peptide bond. This will further have a direct impact on the hydrogen bond between the hydroxyl group of the substrate and the side chain of E435 (see Figure 8, steps A and B). At present, it is not clear how this equilibrium might influence the initial abstraction of the hydrogen atom.

Although the B_{12}-dependent reactions are quite diverse, all of them, except for the ribonucleotide reductase reaction, involve an intramolecular group transfer reaction. In the case of the diol dehydratase reaction mechanism, this involves

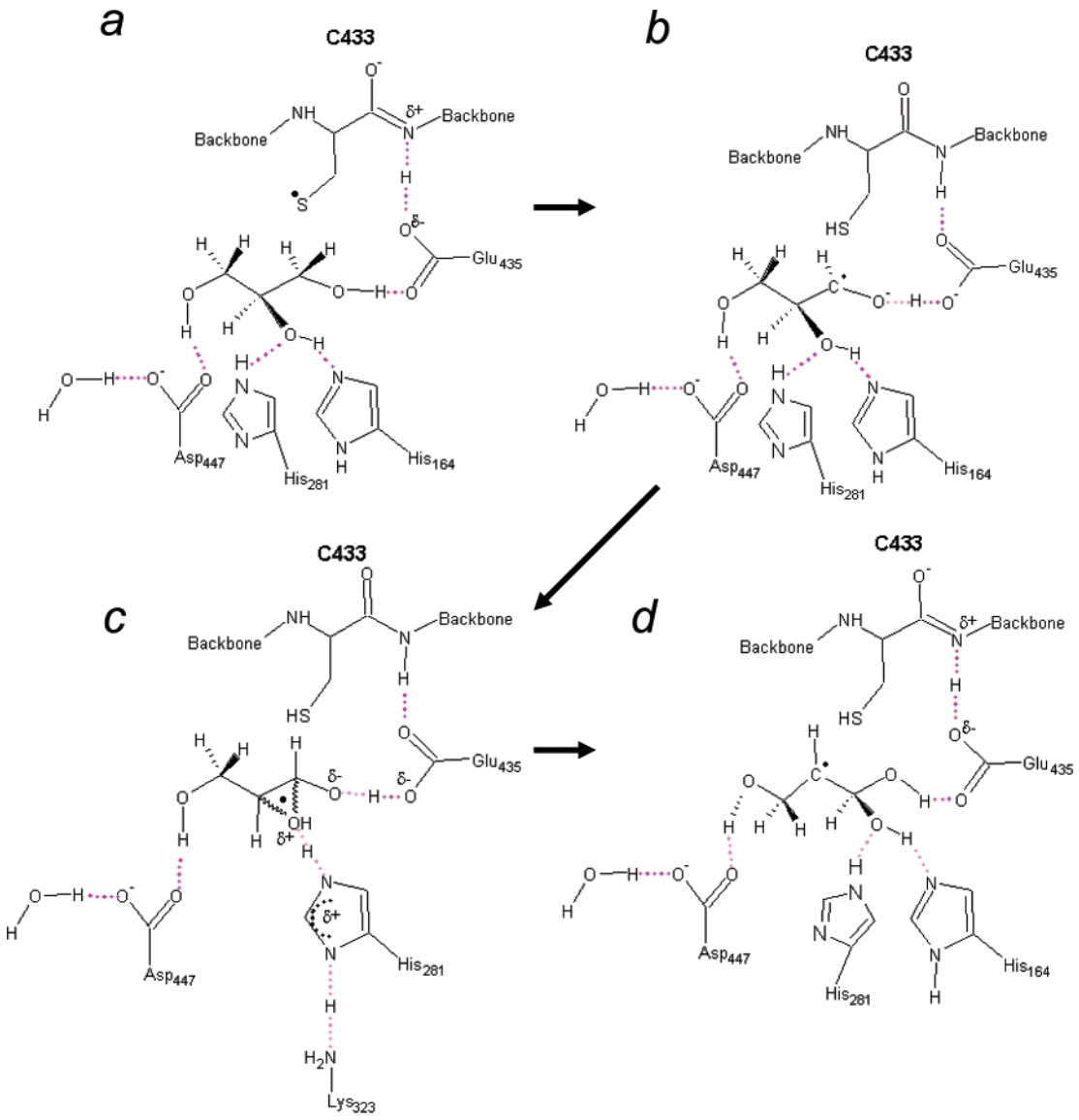

FIGURE 8: Proposed mechanism of vitamin B_{12}-independent glycerol dehydration by the *C. butyricum* glycerol dehydratase.

the overall migration of a hydrogen atom in exchange for the movement of the OH group in the opposite direction. Because of the nature of these reactions, the mechanism of group migrations is difficult to study and has been the subject of considerable debate (recently reviewed in ref *14*). In particular, it is difficult to obtain direct evidence for a specific mechanism from biochemical studies. Therefore, model reactions, X-ray structures, and theoretical calculations have provided significant insight. Of particular interest to this work is the proposal by Golding and Random (*39*) that the barrier in the intramolecular 1,2-shifts of an OH group, through a cyclic transition state, is reduced by protonation of the migrating OH group. A significant problem is that the nature of an acid required to protonate this species would be outside the range of acidic groups found in proteins. Although the active site of an enzyme can modulate pK_a values substantially, the pH at which the enzymes are functioning in general would indicate that the majority of the acidic groups would exist as COO^-, and therefore, the conjugate acids of the active site residues are more likely. A Lewis acid such as K^+ might also lower the energy of this transition state. The latter proposal is consistent with the requirement for potassium in the B_{12}-dependent dehydration of glycerol and the position of K^+ and 1,2-propanediol in the binding site of the B_{12}-dependent glycerol dehydratase model (*35*). In both the glycerol- and 1,2-propanediol-bound forms of the B_{12}-independent GD presented here, we clearly see the interaction of two histidine residues with what would ultimately be the migrating OH group. Because H164 is involved in a hydrogen bond with a backbone carbonyl, it would better serve as the hydrogen bond acceptor for the OH group at C2 of the substrate. H281 is a hydrogen bond acceptor for the side chain amino group of K323 and therefore would be better suited to serve as a conjugate acid for the stabilization of the transition state shown in Figure 8C. The nitrogen atom of H281 is also slightly closer to the migrating OH group in both the glycerol- and 1,2-propanediol-bound structures (2.8 Å compared with 3.0 Å). This mechanism is further supported by computational results that indicate that the presence of imidazolium is effective for transition state stabilization in the absence of K^+ (*40*). For these histidine residues to maintain their interaction with this OH group, the product must reorient itself in the active site. This would essentially amount to a 180° rotation that would place the secondary carbon radical in the proximity of the γ-sulfur atom of C433 (Figure 8D). In this sense, the migration of

the OH group is essential for regeneration of the catalytic radical at the active site. Whether the migration of this OH group is stereospecific, as has been shown for the B_{12}-dependent glycerol and diol dehydratases, remains to be addressed.

Summary. In this work, we present the first isolation and preliminary biochemical characterization of a B_{12}-independent glycerol dehydratase. The 1,2-propanediol dehydratase activity is significantly greater than what has previously been reported for the B_{12}-dependent glycerol and diol dehydratases. We also report the crystal structure for the B_{12}-independent GD and show that it is similar to PFL in both structure and the SAM-dependent activation mechanism. The observation that only the C-terminal domains of PFL and the GD crystal stuctures align, coupled with the observation that a single-point mutation (R782K) in this domain results in the formation of a tight complex *in vivo*, provides support for our hypothesis that this is the binding site for the activating enzyme. Further crystallographic analysis of the binding modes of glycerol and 1,2-propanediol has provided critical insight into the mechanism of B_{12}-independent dehydration reactions. Taken together, the biochemical and structural data presented here provide a solid foundation for a further understanding the B_{12}-independent dehydration reactions and the radical SAM activation mechanism in two-component systems such as PFL.

REFERENCES

1. Frey, P. A. (2003) S-Adenosylmethionine: A wolf in sheep's clothing or a rich man's adenosyl cobalamin, *Chem. Rev. 103*, 2129−2148.
2. Cheek, J., and Broderick, J. B. (2001) Adenosylmethionine-dependent iron−sulfur enzymes: versatile clusters in a radical new role, *J. Biol. Inorg. Chem. 6*, 209−226.
3. Stubbe, J., and van der Donk, W. A. (1998) Protein Radicals in Enzyme Catalysis, *Chem. Rev. 98*, 705−762.
4. Fontecave, M., Mulliez, E., and Ollagnier-de-Choudens, S. (2001) Adenosylmethionine as a source of 5′-deoxyadenosyl radicals, *Curr. Opin. Chem. Biol. 5*, 506−511.
5. Sofia, H. J., Chen, G., Hetzler, B. G., Reyes-Spindola, J. F., and Miller, N. E. (2001) Radical SAM, a novel protein superfamily linking unresolved steps in familiar biosynthetic pathways with radical mechanisms: functional characterization using new analysis and information visualization methods, *Nucleic Acids Res. 29*, 1097−1106.
6. Walsby, C. J., Ortillo, D., Broderick, W. E., Broderick, J. B., and Hoffman, B. M. (2002) An Anchoring Role for FeS Clusters: Chelation of the Amino Acid Moiety of S-Adenosylmethionine to the Unique Iron Site of the [4Fe-4S] Cluster of Pyruvate Formate-Lyase Activating Enzyme, *J. Am. Chem. Soc. 124*, 11270−11271.
7. Layer, G., Moser, J., Heinz, D. W., Jahn, D., and Schubert, W. D. (2003) Crystal structure of coproporphyrinogen III oxidase reveals cofactor geometry of radical SAM enzymes, *EMBO J. 22*, 6214−6224.
8. Frey, M., Rothe, M., Wagner, A. F., and Knappe, J. (1994) Adenosylmethionine-dependent synthesis of the glycyl radical in pyruvate formate-lyase by abstraction of the glycine C-2 pro-S hydrogen atom. Studies of [^{2}H]glycine-substituted enzyme and peptides homologous to the glycine 734 site, *J. Biol. Chem. 269*, 12432−12437.
9. Wagner, A. F., Demand, J., Schilling, G., Pils, T., and Knappe, J. (1999) A dehydroalanyl residue can capture the 5′-deoxyadenosyl radical generated from S-adenosylmethionine by pyruvate formate-lyase-activating enzyme, *Biochem. Biophys. Res. Commun. 254*, 306−310.
10. Miller, H. (2000) Major Fiber Producers Hop on Corterra Bandwagon, *Int. Fiber J. 15*, 14−16.
11. Rudie, R. (2000) Cargill Dow sews seeds of future fibers; Will build 300 million dollar PLA polymer plant, *Int. Fiber J. 15*, 8−12.
12. Sarcabal, P., Croux, C., and Soucaille, P. (2001) Method for preparing 1,3-propanediol with recombinant microorganisms in the absence of coenzyme B12, Patent US2003175916.
13. Emptage, M., Haynie, S., Laffend, L., Pucci, J., and Whited, G. (2001) Process for the Biological Production of 1,3-Propanediol with High Titer, Patent WO0112833.
14. Toraya, T. (2003) Radical catalysis in coenzyme B12-dependent isomerization (eliminating) reactions, *Chem. Rev. 103*, 2095−2127.
15. Toraya, T., Shirakashi, T., Kosuga, T., and Fukui, S. (1976) Substrate specificity of coenzyme B12-dependent diol dehydrase: glycerol as both a good substrate and a potent inactivator, *Biochem. Biophys. Res. Commun. 69*, 475−480.
16. Bachovchin, W. W., Eagar, R. G., Jr., Moore, K. W., and Richards, J. H. (1977) Mechanism of action of adenosylcobalamin: glycerol and other substrate analogues as substrates and inactivators for propanediol dehydratase: kinetics, stereospecificity, and mechanism, *Biochemistry 16*, 1082−1092.
17. Schneider, Z., and Pawelkiewicz, J. (1966) The properties of glycerol dehydratase isolated from *Aerobacter aerogenes*, and the properties of the apoenzyme subunits, *Acta Biochim. Pol. 13*, 311−328.
18. Poznanskaya, A. A., Yakusheva, M. I., and Yakovlev, V. A. (1977) Study of the mechanism of action of adenosylcobalamin-dependent glycerol dehydratase from *Aerobacter aerogenes*. II. The inactivation kinetics of glycerol dehydratase complexes with adenosylobalamin and its analogues, *Biochim. Biophys. Acta 484*, 236−243.
19. Toraya, T., and Mori, K. (1999) A reactivating factor for coenzyme B12-dependent diol dehydratase, *J. Biol. Chem. 274*, 3372−3377.
20. Raynaud, C., Sarcabal, P., Meynial-Salles, I., Croux, C., and Soucaille, P. (2003) Molecular characterization of the 1,3-propanediol (1,3-PD) operon of *Clostridium butyricum*, *Proc. Natl. Acad. Sci. U.S.A. 100*, 5010−5015.
21. Kulzer, R., Pils, T., Kappl, R., Huttermann, J., and Knappe, J. (1998) Reconstitution and characterization of the polynuclear iron−sulfur cluster in pyruvate formate-lyase-activating enzyme. Molecular properties of the holoenzyme form, *J. Biol. Chem. 273*, 4897−4903.
22. Chromy, V., Fischer, J., and Kulhanek, V. (1974) Re-evaluation of EDTA-chelated biuret reagent, *Clin. Chem. 20*, 1362−1363.
23. Otwinowski, Z., and Minor, W. (1997) Processing of X-ray diffraction data collected in oscillation mode, *Methods Enzymol. 276*, 307−326.
24. Potterton, E., Briggs, P., Turkenburg, M., and Dodson, E. (2003) A graphical user interface to the CCP4 program suite, *Acta Crystallogr. D59*, 1131−1137.
25. Jones, T. A., Zou, J. Y., Cowan, S. W., and Kjeldgaard, M. (1991) Improved methods for building protein models in electron density maps and the location of errors in these models, *Acta Crystallogr. A47* (Part 2), 110−119.
26. Brunger, A. T., Adams, P. D., Clore, G. M., DeLano, W. L., Gros, P., Grosse-Kunstleve, R. W., Jiang, J. S., Kuszewski, J., Nilges, M., Pannu, N. S., Read, R. J., Rice, L. M., Simonson, T., and Warren, G. L. (1998) Crystallography & NMR system: A new software suite for macromolecular structure determination, *Acta Crystallogr. D54* (Part 5), 905−921.
27. Kraulis, P. J. (1991) MOLSCRIPT: a program to produce both detailed and schematic plots of protein structures, *J. Appl. Crystallogr. 24*, 945−949.
28. Gouet, P., Robert, X., and Courcelle, E. (2003) ESPript/ENDscript: Extracting and rendering sequence and 3D information from atomic structures of proteins, *Nucleic Acids Res. 31*, 3320−3323.
29. Merritt, E. A., and Bacon, D. J. (1997) *Methods Enzymol. 277*, 505−524.
30. Wagner, A. F., Frey, M., Neugebauer, F. A., Schafer, W., and Knappe, J. (1992) The free radical in pyruvate formate-lyase is located on glycine-734, *Proc. Natl. Acad. Sci. U.S.A. 89*, 996−1000.
31. Henshaw, T. F., Cheek, J., and Broderick, J. B. (2000) The [4Fe-4S]$^+$ Cluster of Pyruvate Formate-Lyase Activating Enzyme Generates the Glycyl Radical on Pyruvate Formate-Lyase: EPR-Detected Single Turnover, *J. Am. Chem. Soc. 122*, 8331−8332.
32. Coschigano, P. W., Wehrman, T. S., and Young, L. Y. (1998) Identification and analysis of genes involved in anaerobic toluene

metabolism by strain T1: putative role of a glycine free radical, *Appl. Environ. Microbiol. 64*, 1650−1656.
33. Hermuth, K., Leuthner, B., and Heider, J. (2002) Operon structure and expression of the genes for benzylsuccinate synthase in *Thauera aromatica* strain K172, *Arch. Microbiol. 177*, 132−138.
34. Toraya, T., Ushio, K., Fukui, S., and Hogenkamp, P. C. (1977) Studies on the mechanism of the adenosylcobalamin-dependent diol dehydrase reaction by the use of analogs of the coenzyme, *J. Biol. Chem. 252*, 963−970.
35. Yamanishi, M., Yunoki, M., Tobimatsu, T., Sato, H., Matsui, J., Dokiya, A., Iuchi, Y., Oe, K., Suto, K., Shibata, N., Morimoto, Y., Yasuoka, N., and Toraya, T. (2002) The crystal structure of coenzyme B12-dependent glycerol dehydratase in complex with cobalamin and propane-1,2-diol, *Eur. J. Biohem. 269*, 4484−4494.
36. Tobimatsu, T., Sakai, T., Hashida, Y., Mizoguchi, N., Miyoshi, S., and Toraya, T. (1997) Heterologous expression, purification, and properties of diol dehydratase, an adenosylcobalamin-dependent enzyme of *Klebsiella oxytoca*, *Arch. Biochem. Biophys. 347*, 132−140.
37. Becker, A., and Kabsch, W. (2002) X-ray Structures of Pyruvate Formate-Lyase in Complex with Pyruvate and CoA, *J. Biol. Chem. 277*, 40036−40042.
38. Reddy, S. G., Wong, K. K., Parast, C. V., Peisach, J., Magliozzo, R. S., and Kozarich, J. W. (1998) Dioxygen inactivation of pyruvate formate-lyase: EPR evidence for the formation of protein-based sulfinyl and peroxyl radicals, *Biochemistry 37*, 558−563.
39. Golding, B. T., and Radom, L. (1976) The mechanism of action of adenosylcobalamin, *J. Am. Chem. Soc. 98*, 6331−6338.
40. Masataka, E., Takashi, K., Yoshizawa, K., and Tetsuo, T. (2002) Theoretical study on the mechanism of catalysis of coenzyme B12-dependent diol dehydratase, *Bull. Chem. Soc. Jpn. 75*, 1469−1481.

BI035930K